Journal of Thermal Science Vol.31, No.6 (2022) 1928−1938

https://doi.org/10.1007/s11630-022-1538-4 **Article ID: 1003-2169(2022)06-1928-11**

Dynamic Research on Cold Storage Performance of a Standard Radiant Floor Cooling System for Office Buildings in Northern China

WANG Xiaolong, MAN Yi, ZHANG Lili, ZHANG Wenke*, ZHANG Linhua*

School of Thermal Engineering, Shandong Jianzhu University, Ji'nan 250101, China

Abstract: Due to the wide application of floor heating systems, the radiant floor cooling systems has developed rapidly in recent years. In this paper, TRNSYS numerical simulation methods are used to study the influence of chilled water supply temperature and flow rate on the cold storage characteristics of a standard floor structure for office buildings in northern China. The results are verified by experimental measurements. The functional relationship between the saturated cold storage time and the chilled water flow rate is quadratic polynomial, while the changes of supply-water temperature have no effect on the saturation time; the supply-water temperature has a linear relationship with the saturated cold storage volume, while the chilled water flow rate has almost no effect on the saturation cold storage volume. The accumulated cold volume of floor changes with time in an exponential distribution with four coefficients, and the floor has the characteristics of rapid cold storage. This paper is instructive for the design, application and promotion of radiant floor cooling systems.

Keywords: radiant floor, cooling, chilled water, saturation time, saturated volume

1. Introduction

In recent years, the concepts and applications related to using floor heating to cool in summer have gradually emerged in northern China. Many office buildings in northern China try to use "floor heating" to heat in winter, and to cool in summer. Floor radiant cooling and heating can use the same laying pipes in floor structure. Cases of using floor radiant cooling have also begun to appear around the world. In Korea, radiant floor heating systems are commonly used in residential buildings, even high-rise houses [1]. Inspired by winter heating, Jeong et al. [1] analyzed the feasibility of radiant floor cooling systems (RFCS) for residential buildings with massive concrete slabs, and found that a RFCS combined with supplementary equipment for dehumidification would satisfy the requirements for cooling. Lee et al. [2] combined the radiant-floor cooling systems with improved fan coil unit, and formed a combined cooling by radiation and convection. Zhang et al. [3] and Xia et al. [4] investigated the performance of lightweight radiant floor cooling combined with underfloor ventilation systems (LRFCUV)，and compared the LRFCUV systems and heavy radiant floor cooling combined with underfloor ventilation systems (HRFCUV). The above research shows that floor radiant cooling technology has good application prospect.

The research on floor radiation in China and abroad mainly focuses on two stages: steady state and non-steady state. In the field of steady state heat transfer,

Special column: Built Thermal Environment GE: DAI Yanjun
Received: May 20, 2021 Corresponding author: ZHANG Linhua; E-mail: zhth0015@sdjzu.edu.cn
ZHANG Wenke zhangwenke@sdjzu.edu.cn

Li et al. [5] analyzed the heat transfer process of radiant floor cooling systems, and proposed the method of equivalent thermal resistance conversion. In addition, Li et al. [6, 7] also proposed a simplified calculation method of floor surface temperature for multi-layer floor structures in radiant floor cooling systems. Based on this analytical solution [7], Wang et al. [8] considered the influence of light and sunlight on the floor surface, and modified the analytical solution of double-layer floor. Zhang et al. [9] developed a simulation model to validate the simplified calculation method of the surface temperature distribution, which yields an error of 8% or less between the simulated and calculated values, and the absolute error of the average surface temperature of floor is 0.5°C or less. Wu et al. [10] proposed to use the shape factor method to solve the floor surface temperature, and gave the calculation steps for radiant floor heating and cooling systems. In the steady-state stage, the research on floor radiant cooling systems mainly focuses on the analysis of heat transfer process and the solution of floor surface temperature distribution.

In the field of non-steady heat transfer, the main research on floor radiant cooling is also divided into two parts: intermittent operation of systems and the energy storage characteristics of the floor. This is because the floor structure has great thermal inertia and hot (cold) storage capacity.

For the intermittent operation of radiant floor cooling systems, Larsen et al. [11] developed an exact 2-D transient solution of a slab with an embedded array of parallel circular pipes for heating and cooling, and obtained the analytical solution. Merabtine et al. [12] proposed a new transient simplified model for radiant heating slab surface temperature and heat transfer rate calculation which can evaluate the slab surface temperature and can examine its dynamic thermal behavior. Joe et al. [13] proposed an intelligent operation predictive model to optimize the performance of radiant floor cooling systems in office buildings, which can save 34% of operating costs during the cooling season. Hassan A. et al. [14] provided an overview of established practices and recent efforts in modeling, simulation, operation, control, and integration of radiant cooling systems with model predictive control that can reduce energy consumption by up to 44%. Lin et al. [15] found that the floor heating systems have good thermal storage performance, which can be used to a night-running model to achieve the purpose of economic saving and "shifting peak load to off-peak".

There are also many studies on the energy storage characteristics of the floor in radiant floor systems. Xu et al. [16] found a novel organic-inorganic composite phase change material (PCM) called disodium hydrogen phosphate dodecahydrate-lauric-palmitic acid (D-LA-PACM) can be used as a feasible material for energy-saving floor units in radiant floor heating systems. Wang et al. [17] obtained the influence of design parameters (pace between pipes, thickness of the filling layer, and pipe water temperature) on the floor heat storage and release by numerical simulation. Xu et al. [18] studied the energy storage and release performance of double phase change floor in radiant floor cooling/heating systems. Mohammadzadeh et al. [19] used PCMs to improve energy storage performance of floor in radiant floor systems that can achieve significant energy savings. Yun et al. [20] analyzed the thermal storage performance of floor using latent heat storage sheets in floor heating systems, and found that it is possible to store thermal energy by using PCMs.

To sum up, the research on the dynamic energy storage characteristics of floor mostly focuses on heat storage and PCMs, while there is little research on the cold storage characteristics of floor structure. The radiant floor cooling systems urgently need research on the law of cold storage of floor. The dynamic characteristics of cold storage of a standard floor structure in radiant floor cooling systems for office buildings are studied in this paper, and the effect of chilled water supply temperature and flow rate on cold storage dynamic law is analyzed by TRNSYS numerical simulation. The results are verified.

2. Physical Model

A 1:1 model is established in TRNSYS software based on the radiant floor laboratory of Shandong Jianzhu University [21] as a prototype. The laboratory is located in the basement, divided into the inner room and outer room, as shown in Fig. 1. The sizes of the two rooms and the materials of envelopes except the floor are shown in

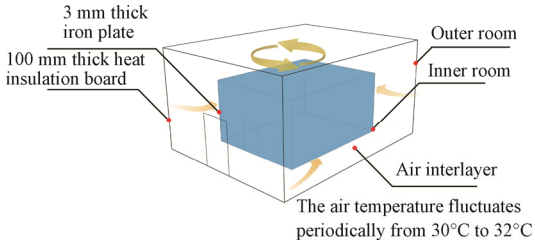

Fig. 1 Schematic diagram of laboratory

Table 1 The size of the inner-outer rooms and the materials of walls

Room	Length	Width	Height	Material of walls
Outer room	5 m	5 m	3.8 m	100 mm thick heat insulation board
Inner room	3.85 m	3.85 m	2.6 m	3 mm thick iron plate

Table 1. The floor is a "floor heating" standard floor structure of office buildings [21], and its surface area is 14.82 m^2. All the data in this paper are based on the floor surface area of 14.82 m^2. There is an air interlayer between the two rooms, and the air interlayer is 0.45 m. The air temperature in the interlayer can be controlled by the air conditioner. In this study, the air temperature in the interlayer is controlled to fluctuate periodically between 30°C to 32°C. The main function of this laboratory is to study the dynamic law of cold storage-release of the standard floor in office buildings.

3. Effect of Supply-Water Temperature on Cold Storage Performance

3.1 Cooling performance on indoor environment

When supply-water temperature is 7°C, 9°C, 11°C and 13°C, the change of indoor air temperature, floor surface temperature and supply-return water temperature with time is shown in Fig. 2.

As shown in Fig. 2(a), the supply-water temperature is low, resulting in a rapid drop in floor surface temperature. As the floor structure stores cold, the temperature difference between the supply and return water decreases, and the system enters steady-state heat transfer period after about 4.25 hours. Due to the heat exchange, the indoor air temperature decreases as the floor surface temperature decreases. The temperature index change trend of Fig. 2(b)–(d) are similar to Fig. 2(a), but with the increase of supply-water temperature, the decrease of floor surface temperature and the indoor air temperature are smaller and smaller.

The above results show that supply-water temperature has a large effect on the surface temperature of floor which will affect the cooling capacity of the floor and the cooling effect on the indoor environment. The lower the supply-water temperature, the better the cooling performance of floor.

3.2 Instantaneous cold release analysis

The essence of the different cooling performance of different supply-water temperatures is that the floor, as a cooling end, has different heat flow released to the indoor environment as shown in Fig. 3(a). "Cold released by the floor" is defined as positive, and "heat released by the floor" is defined as negative.

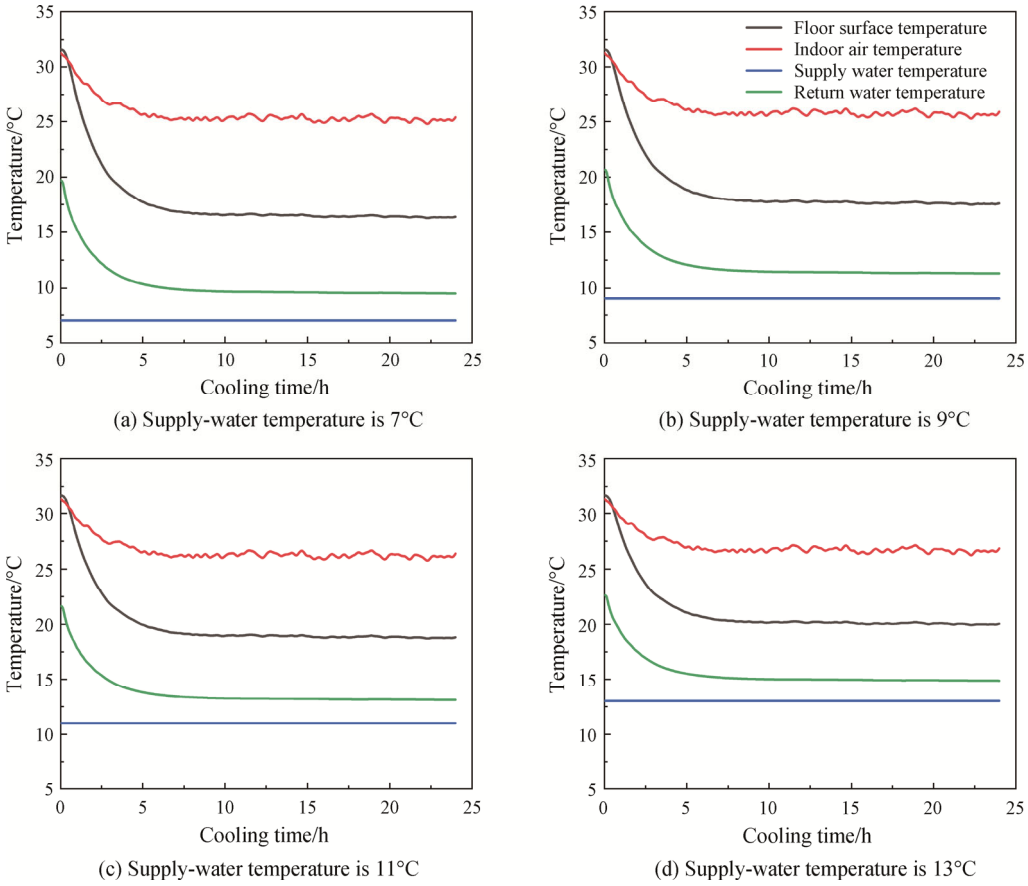

Fig. 2 Temperature index changes of different supply-water temperature

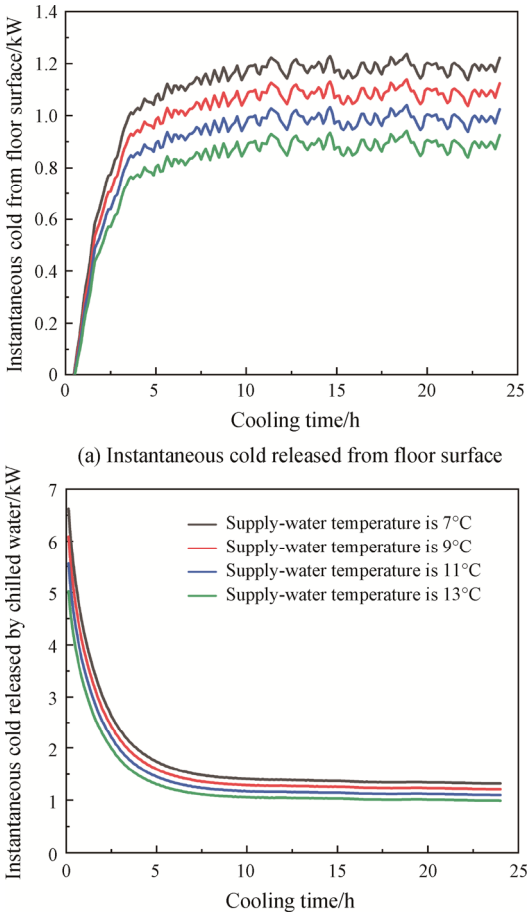

Fig. 3 Effect of supply-water temperature on instantaneous cold

In the radiant floor cooling systems, the cold carried by chilled water in the laying pipes of floor has two destinations. On one hand, the cold is released from the floor surface to cool for indoor environment. On other hand, the cold is used to cool the floor structure; that is the cold is stored in the thermally inert structure. The instantaneous cold storage volume Q_x of floor under the condition of supply-water temperature of x°C can be expressed as the following relation.

$$Q_x = Q_{x,\mathrm{w}} - Q_{x,\mathrm{f}} \tag{1}$$

where, $Q_{x,\mathrm{w}}$ is the total instantaneous cold released by the chilled water of x°C. $Q_{x,\mathrm{f}}$ is the instantaneous cold released by the floor surface to indoor environment.

In Fig. 3(a), it can be seen that the curves under each condition show the same change trend with time. Due to the high initial temperature and large thermal inertia of the floor structure, the cold released has a certain delay of about 0.4 hours. The heat transfer starts with a non-steady state period that most of the cold is stored in the floor and used to cool the floor structure, so the cold released from the floor surface is little. With the increase of cooling time, the cold released from the floor surface gradually increased, and about 4.5 hours later, the cold released curve under each condition is close to a horizontal straight line, fluctuating around a fixed value which indicates that the heat transfer enters steady-state period.

As can be seen in Fig. 3(b), the instantaneous total cold by chilled water tends to decrease as water supply temperature and cooling time increases. The cold released by supply-water temperature of 7°C is significantly higher than supply-water temperature of 13°C. The curves in Fig. 3(b) have big drop at the beginning of cooling, and finally tend to a horizontal straight line, which is due to a large volume of cold is stored in the floor at beginning. When the storage of cold close to saturation, the cold released by chilled water is almost all used for indoor cooling.

3.3 Accumulated storage cold volume

After calculation, the instantaneous cold storage volumes under different supply-water temperature conditions are obtained, as shown in Fig. 4(a). During cooling, the floor structure is cooled down, that process is to store cold in the floor structure continuously. The

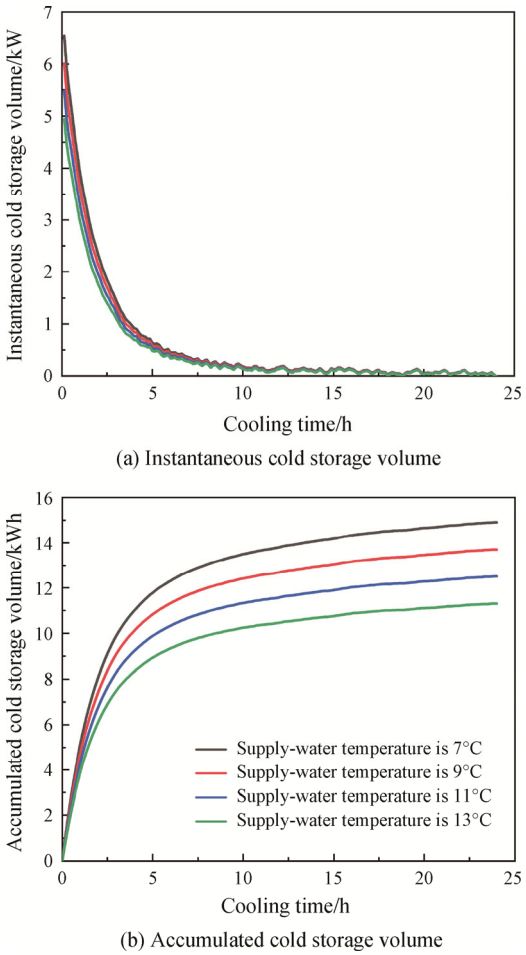

Fig. 4 Effect of water-supply temperature on cold storage volume

accumulated storage cold volume can be obtained by integrating the instantaneous cold storage volume $Q_{x,k}$ by time:

$$E_{x,k} = \int_0^k Q_{x,k} \mathrm{d}t \tag{2}$$

where, $E_{x,k}$ is the accumulated cold storage volume of x°C supply-water at k-th moment, referred to as "accumulated cold volume", and the unit is kWh. The accumulated cold volume of floor changes with time under each condition are shown in Fig. 4(b).

As shown in Fig. 4(b), the accumulated storage cold volume curves under each conditions show similar change trend, growing rapidly at beginning then entering slow growth stage, and finally approaching to a horizontal straight line which indicates that the process of storage cold to floor is close to saturation state.

The variation law of the accumulated cold volume of floor with time under each conditions conform to the exponential model: $f(k) = A \cdot \mathrm{e}^{(b \cdot k)} + C \cdot \mathrm{e}^{(d \cdot k)}$. The equation has four parameters of A, b, C, d.

The fitting functions of the curves in Fig. 4(b) under each condition are obtained, as shown below. The function fitting curves of the sample points are presented in Fig. 5, and the coefficient of determination R^2 are all above 0.99, indicating a good degree of fit.

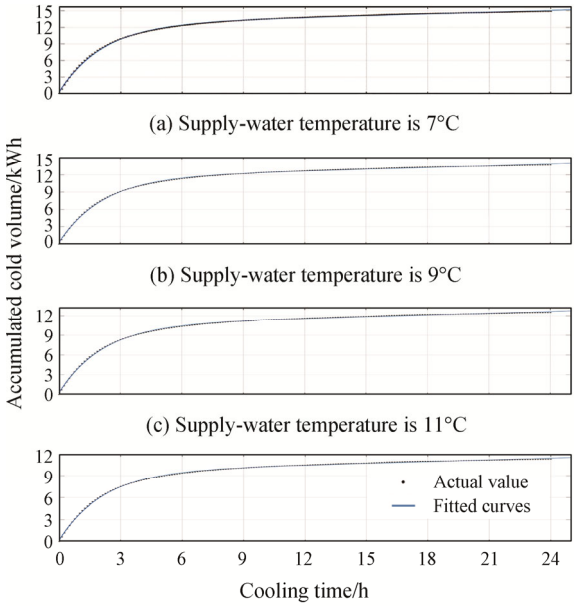

Fig. 5 Accumulated storage cold volume of floor with time

When supply-water temperature is 7°C, the fitting function in Fig. 5(a) is:

$$f(7,k) = 12.65\mathrm{e}^{(0.007\,331k)} - 12.32\mathrm{e}^{(-0.4627k)} \tag{3}$$

When supply-water temperature is 9°C, the fitting function in Fig. 5(b) is:

$$f(9,k) = 11.63\mathrm{e}^{(0.007\,331k)} - 11.33\mathrm{e}^{(-0.4626k)} \tag{4}$$

When supply-water temperature is 11°C, the fitting function in Fig. 5(c) is:

$$f(11,k) = 10.61\mathrm{e}^{(0.007\,313 \cdot k)} - 10.3\mathrm{e}^{(-0.4624 \cdot k)} \tag{5}$$

When supply-water temperature is 13°C, the fitting function in Fig. 5(d) is:

$$f(13,k) = 9.595\mathrm{e}^{(0.007\,302 \cdot k)} - 9.354\mathrm{e}^{(-0.4622 \cdot k)} \tag{6}$$

From the coefficients of Eqs. (3)–(6) above, it can be seen that b and d are almost constant, independent of the changes of supply-water temperature. When the floor structure is determined, the coefficients b and d are also determined. The two coefficients b and d are defined as "structure coefficients" which are determined by floor structure. For the standard floor structure, b is 0.0073 and d is –0.4624. It also can be seen from Eqs. (3)–(6), the coefficients A and C change proportionally to the the supply-water temperature. The coefficients A and C can be written as the unit area coefficients a and c multiplied by the floor surface area S. The coefficients a and c are linearly related to the supply-water temperature, as shown in Fig. 6. These two coefficients determined by supply-water temperature are defined as "temperature coefficients". The values of coefficient a and c per unit area can be obtained by checking Fig. 6 according to the current supply-water temperature.

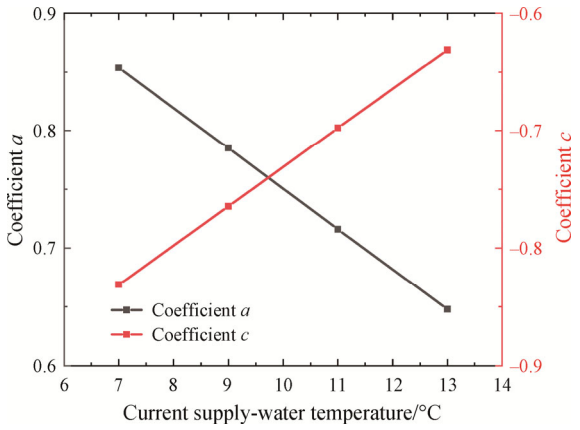

Fig. 6 The values of coefficients a and c for different supply-water temperature

When the two structure coefficients b and d and two temperature coefficients a and c are determined, the accumulated cold volume of the floor changes with time are also determined, as Eq. (6).

$$E_{x,k} = \left(a \cdot \mathrm{e}^{b \cdot k} + c \cdot \mathrm{e}^{d \cdot k}\right) \cdot S \tag{7}$$

where, k should take the date of hour as unit to participate calculation, and S is floor surface area and should take the date of m^2 as unit to participate calculation. If Eq. (7) is not multiplied by S, it represents

the cold storage volume of the floor structure per unit area, and multiplied by S represents the cold storage volume of the entire floor area. For non-standardized floor structures, the floor structure parameters need to be input into the TRNSYS software to obtain the non-standardized values of b and d.

3.4 Saturation time and saturated cold storage volume

Due to the consistent existence of temperature difference between chilled water and floor structure, floor cold storage can only be infinitely close to saturation state, and there is no real saturation point. To facilitate analysis, the saturation state is defined that the first moment when the growth rate of cold storage volume is less than 1%, as shown in Eq. (8).

$$\frac{E_{x,j+1}-E_{x,j}}{E_{x,j}}<1\% \tag{8}$$

If the j-th moment is the first moment that satisfies the above formula, the j-th moment can be considered to reach saturation state and the saturation time is j with the the unit hour. At j-th moment, the corresponding accumulated cold volume of floor at time j-th is the saturated cold storage volume $E_{x,j}$.

After calculations, the curves of the growth rate of accumulated cold storage volume under each condition are obtained as shown in Fig. 7.

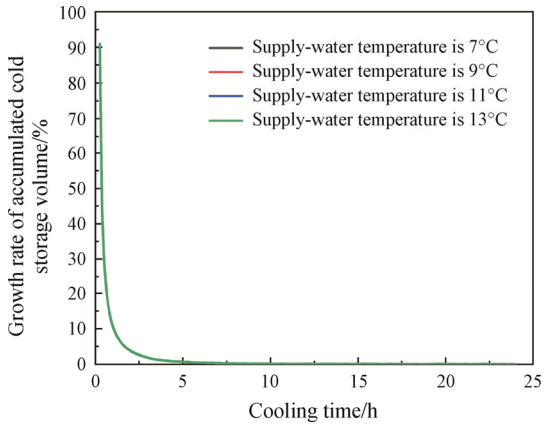

Fig. 7 The growth rate of accumulated cold volume

It can be seen that the curves in each condition coincide into one, which indicates that the growth rate of each condition follows the same growth law, no matter what the supply-water temperature is. The growth rate of floor storage cold is independent of the supply-water temperature. At the beginning of cooling, the floor cold storage speed is very fast, and at about 1.75 hours, it turns and the growth rate becomes very slow. Eventually, the growth rate approaches to 0.

The time to cold storage saturation state is 4.25 hours for all conditions, as shown in Fig. 8.

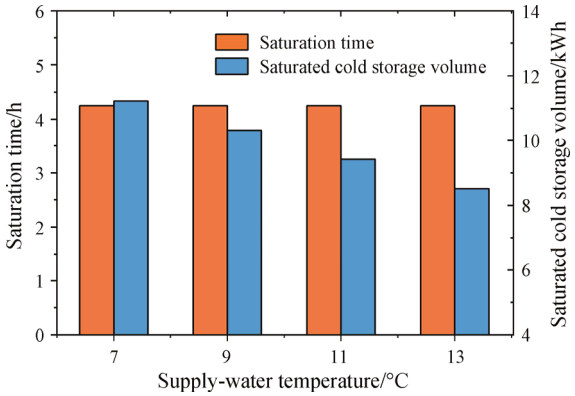

Fig. 8 Saturation time and saturated cold storage volume

Fig. 8 shows that the variation of the supply-water temperature has no effect on the saturation time of the cold storage of floor.

When the floor cold storage reaches saturation state, the saturated cold storage volume of each condition is also shown in Fig. 8. When the chilled water supply temperature is 7°C, the maximum volume of cold stored is 11.23 kWh. As the supply-water temperature rises, the volume of cold in the saturation state gradually decreases. When the chilled water temperature is 13°C, the saturated cold storage volume is only 8.45 kWh. Using the least square method, the fitting relationship between saturated cold storage volume and supply-water temperature is obtained as shown in Fig. 9.

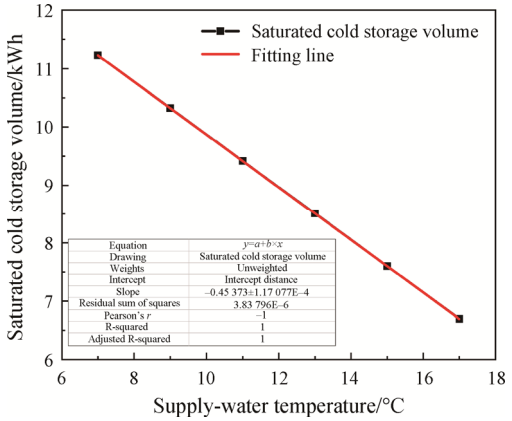

Fig. 9 Fitting relationship between saturated cold volume and water supply temperature

From Fig. 9, it can be seen that the saturated storage cold volume of floor and the supply-water temperature are linearly related with a very good fit. The higher the supply-water temperature, the lower the saturated cold storage volume. In practice, we can increase the storage cold volume of floor by reducing the chilled water supply temperature.

Through the above analysis, it is found that the floor also has the characteristics of rapid cold storage. Taking

one day (24 hours) as the research cycle and the supply-water temperature of 7°C as the research example, we found that the cold storage volume of floor is 8.076 kWh in the first 2 hours, accounting for 54.19% of the total cold storage volume of whole 24 hours, and in 3.5 hours of cooling, the storage cold volume has reached 70.56%. This shows that the early opening of the floor cooling systems will store a large volume of cold. But more than 3.5 hours, the efficiency of cold storage becomes extremely low, and a long time to open the cooling systems is not conducive to the storage of cold.

4. Effect of Chilled Water Flow on Cold Storage Performance

4.1 Cooling effect of chilled water flow on indoor thermal environment

The chilled water supply temperature is selected as 13°C, and the influence of chilled water flow on the indoor thermal environment is studied by changing the water flow rate through the laying pipes of floor as 270 kg/h, 490 kg/h, 630 kg/h and 810 kg/h. The temperature index changes are shown in Fig. 10.

As can be seen in Fig. 10(b), the temperature drops of floor surface temperature, room air temperature, and return water are approximately equal to that at 270 kg/h flow rate. The inflection point of temperature change is earlier than Fig. 10(a). The temperature drop of indoor air and floor surface in Fig. 10(c) is almost the same as in Fig. 10(b), but the temperature inflection point is earlier than that. The inflection point of Fig. 10(d) is earlier than that of Fig. 10(c), but the advance is not obvious. The changes of chilled water flow will affect the time to enter steady-state heat transfer, and the faster the chilled water flow rate, the sooner.

4.2 Instantaneous cold release analysis

The instantaneous cold released from the floor surface and by chilled water of different flow rate is shown in Fig. 11.

As can be seen from Fig. 11(a), the four curves overlap to a high degree. As the chilled water flow increases, the inflection point of the curves becomes more obvious and earlier. The difference is obvious between the curves of 270 kg/h and the flow rate of 450 kg/h, but it is not obvious for the two curves of 630 kg/h and 810 kg/h which almost coincide. This phenomenon shows that in low flow rate zone, changing the chilled

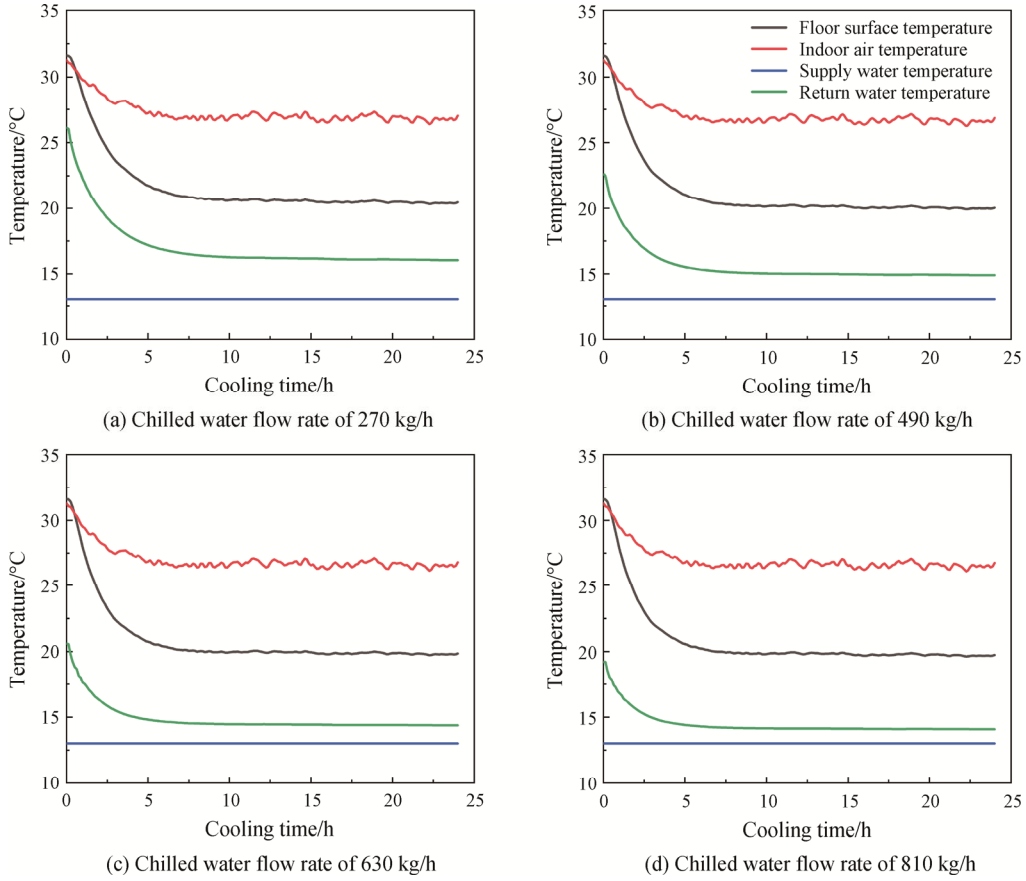

(a) Chilled water flow rate of 270 kg/h

(b) Chilled water flow rate of 490 kg/h

(c) Chilled water flow rate of 630 kg/h

(d) Chilled water flow rate of 810 kg/h

Fig. 10 Effect of chilled water flow on indoor environment

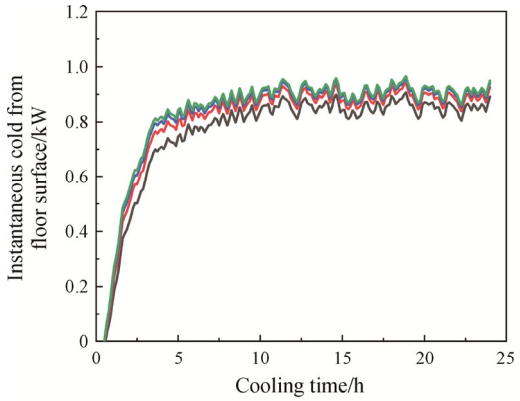

(a) Instantaneous cold released from the floor surface

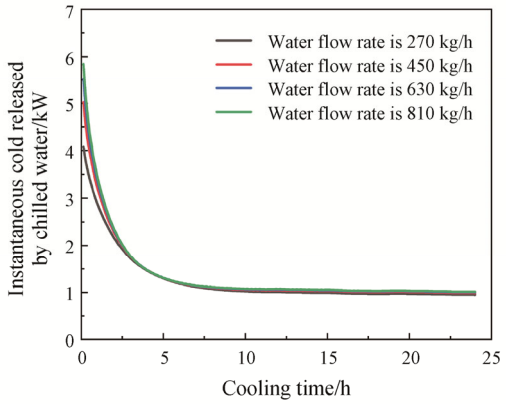

(b) Instantaneous cold released by chilled water

Fig. 11 Effect of chilled water flow rate on instantaneous cold

water flow rate has a greater impact on the cooling effect of floor, while in high flow rate zone, changing the chilled flow rate has almost no effect.

For Fig. 11(b), the four curves have a higher degree of overlap. The curve of chilled water flow rate at 810 kg/h and the curve of 630 kg/h almost overlap as one curve. The difference between the four curves only lies in the initial stage of cooling, and the faster the chilled water flow, the larger the instantaneous cold volume released by chilled water will be.

4.3 Accumulated storage cold volume

The instantaneous cold volume stored inside the floor is that the total cold volume entering the floor structure minus the cold volume released from the surface of floor. By calculations, the instantaneous cold storage volume under each condition is shown in Fig. 12(a). By integrating the instantaneous cold storage volume with time, the accumulated cold storage volume of the floor can be obtained, as shown in Fig. 12(b).

Fig. 12(a) shows that the curves of instantaneous cold storage volume of floor almost overlap into one curve. The four curves differ only at the beginning of cooling. For Fig. 12(b), the change curves of accumulated cold storage at chilled water flow rate of 810 kg/h and 630 kg/h basically overlap, but other curves are obviously different. This is because that 630 kg/h is the critical flow rate, and the chilled water flow rate exceeding the critical speed will not contribute to the cold storage capacity of floor. Fig. 12(b) also shows that with the decrease of cold water flow, the curve becomes smoother, and with the increase of cold water flow, the curve "inflection point" is more obvious and the time point of inflection will be more advanced.

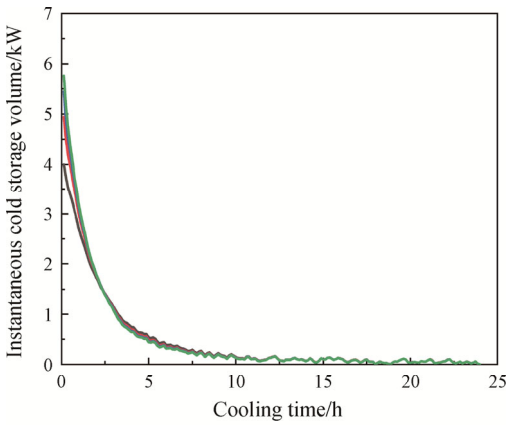

(a) Instantaneous cold storage volume

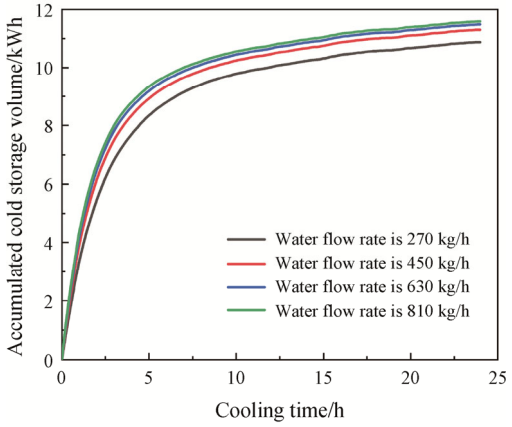

(b) Accumulated cold storage volume

Fig. 12 Effect of chilled water flow rate on the cold storage volume

This shows that the flow rate of chilled water has a positive effect on the early saturation state of storage cold, and the higher the flow rate, the shorter the time to reach saturation.

4.4 Saturation time and saturated cold storage volume

Again, the saturation time and saturated cold storage capacity are calculated by taking "the growth rate of accumulated cold storage volume of floor for the first time is less than 1%" as an indicator. The results are shown in Fig. 13.

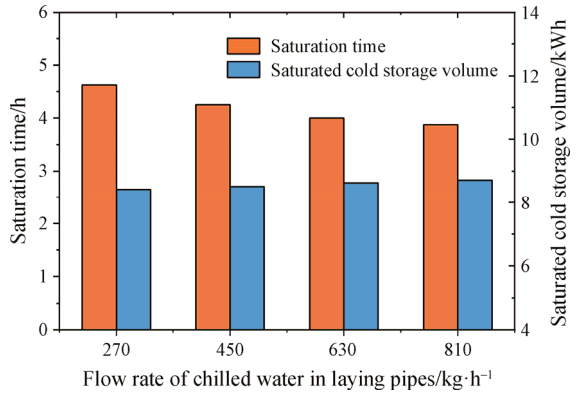

Fig. 13 Saturation time and saturated cold storage volume

Fig. 13 shows that when the chilled water flow rate is 270 kg/h, the time of saturation is 4.63 hours. When the chilled water flow rate is 450, 630 and 810 kg/h respectively, the corresponding saturation time is 4.25, 4.00 and 3.88 h. The saturation time of the flow rate at 810 kg/h is nearly 1 hour earlier than that of the flow rate at 270 kg/h. This shows that the higher the flow rate, the easier it is for the floor to reach cold storage saturation state, but the saturation time does not change proportionally with the flow rate, and these two conform to the following fitting relationship:

$$T_b = 2\times10^{-6}M^2 - 0.0034M + 5.41 \quad (9)$$

where, T_b is the saturation time with unit hour, and M is the mass flow which should take the value of kg/h as unit to participate calculation.

The extreme point of Eq. (9) is located in the high-speed flow rang, which also explains that changing the flow in high-speed flow rang has little effect on the saturation time, while the low-speed flow rang is far away from the extreme point, and changing the flow has a great effect on the saturation time. In practice, the saturation time can be corrected by Eq. (9) according to the actual chilled water flow.

The saturated cold storage volume of each condition is also shown in Fig. 13. When the floor structure reaches cold storage saturation state, the accumulated cold storage volume is almost equal, especially the last two histograms. This shows that when the supply-water temperature remains constant, the chilled water flow rate has little effect on the saturated cold storage volume, especially when the chilled water flow rate is high.

5. Verification

For the validation of numerical simulation calculation, the Shandong Jianzhu University [21] radiant floor cooling/heating laboratory is used for actual measurement. The water-supply temperature is selected as 13°C, and the flow rate is selected as 450 kg/h for the verified operating conditions. The numerical simulation results are compared with the experimental results in Fig. 14.

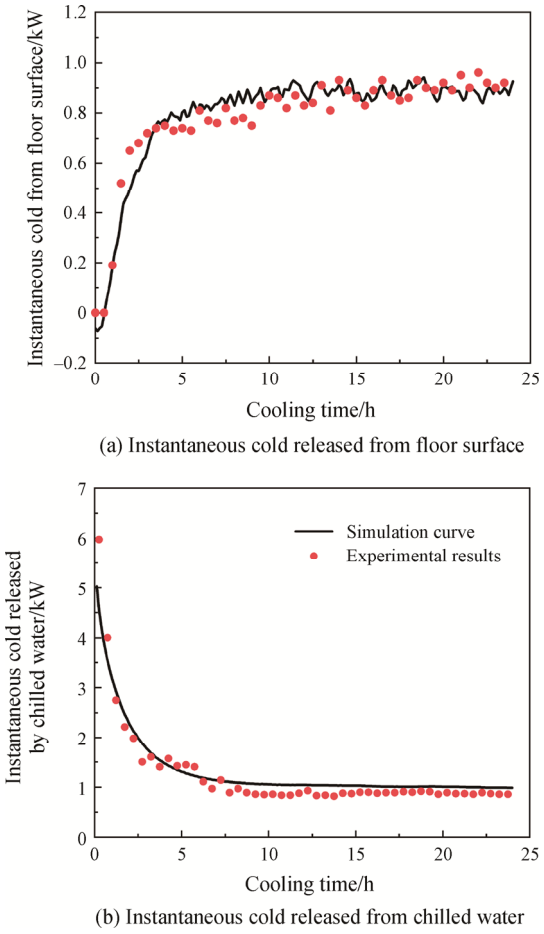

Fig. 14 Comparison of simulation results with experimental results

Fig. 14 shows that there is a good agreement between the simulated curve and the experimental measured data. The trend of the measured discrete data is exactly the same as the trend of simulated curve, and although there are errors, there is a high degree of overlap between the two. From Fig. 14, at the beginning of cooling, the measured date has a deviation from the simulated curve. At this time, the measured data is inaccurate, and invalid. About 0.5 hour later, the discrete data is normal. The maximum deviation of Fig. 14(a)–(b) both occurs at the turning of simulated curves. The maximum relative error is within 25%.

The above comparison results prove the reasonableness of numerical simulation and the correctness of parameter settings in TRNSYS, and also ensure the accuracy of the results in this study.

6. Conclusions

The dynamic characteristics of cold storage of a standard floor structure for office buildings are discussed in this paper. The main conclusions are summarized as follows:

(1) The supply-water temperature plays a main role on cooling effect and storage cold volume of floor, which determines the "amount" of cold storage. The chilled water flow rate mainly plays a role in the cold storage time, which determines the "fast and slow" of cold storage.

(2) The change law of accumulated cold storage volume of floor with time is exponential distribution with four coefficients. The floor has the characteristics of rapid cold storage, which will store more than 70% of total cold storage volume in first 15% of the 24 hours.

(3) The relationship between the saturation cold storage time of floor and the chilled water flow in the laying pipes is parabolic, and its extreme point is located in the high-speed flow range.

The conclusions have guiding significance for the design, application and promotion of radiant floor cooling systems.

Acknowledgements

This study is financially supported by the Plan of Guidance and Cultivation for Young Innovative Talents of Shandong Provincial Colleges and Universities, and is financially supported by the National Natural Science Foundation of China (Grant No. 51808321).

References

[1] Jeong C.H., Yeo M.S., Kim K.W., Feasibility of a radiant floor cooling system for residential buildings with massive concrete slab in a hot and humid climate. International Journal of Concrete Structures and Materials, 2018, 12(1): 1–14.

[2] Lee K.G., Hong W.H., Thermal-environment characteristics and comfort of combined radiant-floor (Korean heating system ondol) and convective cooling system. Journal of Central South University, 2013, 20(12): 3589–3603.

[3] Zhang D., Cai N., Rui Y., Tang H., Liu M., Experimental study on performance comparison between heavy and lightweight radiant floor cooling combined with underfloor ventilation air conditioning system. Proceedings of the 8th International Symposium on Heating, Ventilation and Air Conditioning, Berlin, Heidelberg, 2014, 262: 475–483.

[4] Xia X.Y., Zhang X., Experimental study on performance of lightweight radiant floor cooling combined with underfloor ventilation system. Low-carbon City and New-type Urbanization, 2015, pp: 307–315.

[5] Li Q.Q., Chen C., Zhang Y., Lin J., Ling H.S., Simplified thermal calculation method for floor structure in radiant floor cooling system. Energy and Buildings, 2014, 74: 182–190.

[6] Li Q.Q., Zhang Y., Guo T.M., Fan J.H., Development of a new method to estimate thermal performance of multilayer radiant floor. Journal of Building Engineering, 2021, 33: 101562.

[7] Li Q.Q., Chen C., Zhang Y., Lin J., Ling H.S., Ma Y., Analytical solution for heat transfer in a multilayer floor of a radiant floor system. Building Simulation, 2014, 7(3): 207–216.

[8] Wang X.L., Zhang W.Q, Li Q.Q, Zhang W.K., Lei W.J, Zhang L.H., An analytical method to estimate temperature distribution of typical radiant floor cooling systems with internal heat radiation. Energy Exploration & Exploitation, 2021, 39(4): 1283–1305.

[9] Zhang L., Liu X.H., Jiang Y., Simplified calculation for cooling/heating capacity, surface temperature distribution of radiant floor. Energy and Buildings, 2012, 55: 397–404.

[10] Wu X.Z, Zhao J.N, Olesen B.W., Fang L., Wang F.H., A new simplified model to calculate surface temperature and heat transfer of radiant floor heating and cooling systems. Energy and Buildings, 2015, 105: 285–293.

[11] Larsen S.F., Filippín C., Lesino G., Transient simulation of a storage floor with a heating/cooling parallel pipe system. Building Simulation, 2010, 3(2): 105–115.

[12] Merabtine A., Mokraoui S., Kheiri A., Dars A., New transient simplified model for radiant heating slab surface temperature and heat transfer rate calculation. Building Simulation, 2019, 12(3): 441–452.

[13] Joe J., Karava P., A model predictive control strategy to optimize the performance of radiant floor heating and cooling systems in office buildings. Applied Energy, 2019, 245: 65–77.

[14] Hassan M.A., Abdelaziz O., Best practices and recent advances in hydronic radiant cooling systems – Part II: Simulation, control, and integration. Energy and Buildings, 2020, 224: 110263.

[15] Lin Z.G., Zhang S.Y., Fu X.Z., Wang Y., Investigation of floor heating with thermal storage. Journal of Central South University of Technology, 2006, 13(4): 399–403.

[16] Xu Q., Akkurt N., Zou Z.W., Liu Y., Feng J.X., Yu C.Q., Ding C., Xiong Y.X., Zhou J.Z., Zang Y., Ding Y.L., Synthesis and characterization of disodium hydrogen phosphate dodecahydrate-lauric-palmitic acid used for indoor energy storage floor units. Journal of Thermal Science, 2020, 29(2): 477–485.

[17] Wang D., Liu Y., Wang Y., Liu J., Numerical and

experimental analysis of floor heat storage and release during an intermittent in-slab floor heating process. Applied Thermal Engineering, 2014, 62(2): 398–406.

[18] Xu Y., Sun B.B., Liu L.J., Liu X.Y., The numerical simulation of radiant floor cooling and heating system with double phase change energy storage and the thermal performance. Journal of Energy Storage, 2021, 40: 102635.

[19] Mohammadzadeh A., Kavgic M., Multivariable optimization of PCM-enhanced radiant floor of a highly glazed study room in cold climates. Building Simulation, 2020, 13(3): 559–574.

[20] Yun B.Y., Yang S., Cho H.M., Wi S., Kim S., Thermal storage effect analysis of floor heating systems using latent heat storage sheets. International Journal of Precision Engineering and Manufacturing-Green Technology, 2019, 6(4): 799–807.

[21] Wei Z.Q., Wang X.L., Zhang W.K., Zhang L.L., Zhang L.H., Floor radiation & fresh air coupled cooling laboratory design and cold storage research. Journal of Northeast Dianli University, 2021, 41(2): 48–54. (in Chinese)